
A Parallel Monolithic Domain Decomposition Method for Blood Flow Simulations in 3D

Yuqi Wu¹ and Xiao-Chuan Cai²

¹ Department of Applied Mathematics, University of Colorado at Boulder, Boulder, CO
80309, USA, yuqi.wu@colorado.edu

² Department of Computer Science, University of Colorado at Boulder, Boulder, CO 80309,
USA, cai@cs.colorado.edu

Summary. We develop a parallel scalable domain decomposition method for the simulation of blood flows in compliant arteries in 3D, by using a fully coupled system of linear elasticity equation and incompressible Navier-Stokes equations. The system is discretized with a finite element method on unstructured moving meshes and solved by a Newton-Krylov algorithm preconditioned with an overlapping additive Schwarz method. We focus on the accuracy and parallel scalability of the algorithm, and report the parallel performance and robustness of the proposed approach by some numerical experiments carried out on a supercomputer with a large number of processors and for problems with millions of unknowns.

1 Introduction

Computer modeling of fluid-structure interaction (FSI) is a useful tool for the study of hemodynamics of blood flows in human arteries. Accurate modeling helps the prediction and treatment of, for example, vascular diseases. FSI problems are in general difficult to study. One of the main challenges is the effective coupling of the fluid and the structure. Two well-known formulations are iterative and monolithic. In iterative approaches, the fluid and the structure equations are solved one after the other repeatedly, until some desired tolerance is reached [7, 10]. The convergence of these approaches is difficult to achieve in some situations [6], since the approaches are very similar to nonlinear Gauss-Seidel with two large blocks. In contrast, we develop a monolithic coupling similar to [2–4], where the fluid and the structure equations are solved simultaneously in a fully coupled fashion and the coupling conditions are enforced strongly as part of the system. The monolithic approach has been shown to be more robust. Many of the convergence problems encountered within the iterative approaches can be avoided.

With the rapid advancement in high performance computing technologies, high resolution blood flow simulations are expected to provide more details of the physics of blood flows and the artery walls. To obtain highly accurate solutions on a very fine mesh, the parallel performance and scalability of the solution algorithm is becoming

a key issue in the simulation. In [2, 3], a class of parallel scalable Newton-Krylov-Schwarz method was introduced for FSI in 2D. In this paper, we focus on solving the fully coupled FSI system in 3D and also discuss the parallel performance and robustness of the algorithms. The rest of the paper is organized as follows. In Sect. 2, we describe the formulation and the discretization of the fully coupled FSI problem. In Sect. 3, we present the Newton-Krylov-Schwarz method for solving the fully coupled nonlinear system. In Sect. 4, we first validate the method by comparing solutions obtained with the new approach with published results for a straight cylinder problem, then report the parallel performance of the algorithm. Finally, we provide some concluding remarks in Sect. 5.

2 Mathematical Formulation and Discretization

Our fully coupled approach can be described by the coupling of three components, the linear elasticity equation for the wall structure in the reference Lagrangian frame, the incompressible Navier-Stokes equations for the fluid in the arbitrary Lagrangian-Eulerian (ALE) framework, and the Laplace equation for the displacement of the fluid domain.

Let $\Omega_s \in R^3$ be the structure domain. The displacement \mathbf{x}_s of the artery walls is described by

$$\rho_s \frac{\partial^2 \mathbf{x}_s}{\partial t^2} - \nabla \cdot \boldsymbol{\sigma}_s = \mathbf{f}_s \quad \text{in } \Omega_s, \tag{1}$$

where ρ_s is the density of the structure, and $\boldsymbol{\sigma}_s = \lambda_s (\nabla \cdot \mathbf{x}_s) \mathbf{I} + \mu_s (\nabla \mathbf{x}_s + \nabla \mathbf{x}_s^T)$ is the Cauchy stress tensor. The Lamé parameters λ_s and μ_s are related to the Young's modulus E and the Poisson ratio ν_s by $\lambda_s = \nu_s E / ((1 + \nu_s)(1 - 2\nu_s))$ and $\mu_s = E / (2(1 + \nu_s))$. We fix the structure displacement $\mathbf{x}_s = 0$ on the inlet and outlet boundary Γ_s , and apply the zero normal traction condition $\boldsymbol{\sigma}_s \cdot \mathbf{n} = 0$ on the external boundaries.

In order to model the fluid in a moving domain $\Omega_f(t) \in R^3$, the displacement of the fluid domain \mathbf{x}_f in the reference configuration $\Omega_0 \in R^3$ is assumed to satisfy a Laplace equation,

$$\Delta \mathbf{x}_f = 0 \quad \text{in } \Omega_0.$$

We define an ALE mapping A_t from Ω_0 to $\Omega_f(t)$:

$$A_t : \Omega_0 \rightarrow \Omega_f(t), \quad A_t(\mathbf{Y}) = \mathbf{Y} + \mathbf{x}_f(\mathbf{Y}), \quad \forall \mathbf{Y} \in \Omega_0,$$

where \mathbf{Y} is referred to as the ALE coordinates. The incompressible Navier-Stokes equations defined on the moving domain $\Omega_f(t)$ are written in the ALE form as

$$\begin{aligned} \rho_f \frac{\partial \mathbf{u}_f}{\partial t} \Big|_{\mathbf{Y}} + \rho_f [(\mathbf{u}_f - \boldsymbol{\omega}_g) \cdot \nabla] \mathbf{u}_f &= \nabla \cdot \boldsymbol{\sigma}_f && \text{in } \Omega_f(t), \\ \nabla \cdot \mathbf{u}_f &= 0 && \text{in } \Omega_f(t), \end{aligned}$$

where ρ_f is the fluid density, \mathbf{u}_f is the fluid velocity, and $\boldsymbol{\sigma}_f = -p_f I + \mu_f (\nabla \mathbf{u}_f + \nabla \mathbf{u}_f^T)$ is the Cauchy stress tensor. $\boldsymbol{\omega}_g = \partial \mathbf{x}_f / \partial t$ is the velocity of the moving domain and \mathbf{Y} indicates that the time derivative is taken with respect to the ALE coordinates. On the inlet boundary Γ_i , a given velocity profile is prescribed. On the outlet boundary Γ_o , the zero traction condition $\boldsymbol{\sigma}_f \cdot \mathbf{n} = 0$ is considered, where \mathbf{n} is the unit outward normal. These boundary conditions may be chosen differently, depending on the problem at hand.

More importantly, three coupling conditions are strongly enforced on the fluid-structure interface Γ_w

$$\boldsymbol{\sigma}_s \cdot \mathbf{n}_s = -\boldsymbol{\sigma}_f \cdot \mathbf{n}_f, \quad \mathbf{u}_f = \frac{\partial \mathbf{x}_s}{\partial t}, \quad \mathbf{x}_f = \mathbf{x}_s, \quad (2)$$

where $\mathbf{n}_s, \mathbf{n}_f$ are unit normal vectors on the fluid-structure interface.

By introducing the structure velocity $\dot{\mathbf{x}}_s$ as an additional unknown variable, we can rewrite the structure momentum equation (1) as a first-order system of equations. We define the variational space of the structure problem as

$$X = \{ \mathbf{x}_s \in [H^1(\Omega_s)]^3 : \mathbf{x}_s = 0 \text{ on } \Gamma_s \}. \quad (3)$$

The weak form of the structure problem is stated as follows: Find $\mathbf{x}_s \in X$ and $\dot{\mathbf{x}}_s \in X$ such that $\forall \phi_s \in X$ and $\forall \varphi_s \in X$,

$$\begin{aligned} B_s(\{ \mathbf{x}_s, \dot{\mathbf{x}}_s \}, \{ \phi_s, \varphi_s \}; \boldsymbol{\sigma}_f) &= \rho_s \frac{\partial}{\partial t} \int_{\Omega_s} \dot{\mathbf{x}}_s \cdot \phi_s \, d\Omega + \int_{\Omega_s} \nabla \phi_s : \boldsymbol{\sigma}_s \, d\Omega \\ &- \int_{\Gamma_w} \phi_s \cdot (\boldsymbol{\sigma}_f \cdot \mathbf{n}_s) \, ds - \int_{\Omega_s} \mathbf{f}_s \cdot \phi_s \, d\Omega + \int_{\Omega_s} \left(\frac{\partial \mathbf{x}_s}{\partial t} - \dot{\mathbf{x}}_s \right) \cdot \varphi_s \, d\Omega = 0. \end{aligned}$$

The variational spaces of the fluid subproblem are time dependent, and the solution of the structure subproblem provides an essential boundary condition for the fluid subproblem by (2). We define the trial and weighting function spaces as:

$$\begin{aligned} V &= \{ \mathbf{u}_f \in [H^1(\Omega_f(t))]^3 : \mathbf{u}_f = g \text{ on } \Gamma_i, \mathbf{u}_f = \partial \mathbf{x}_s / \partial t \text{ on } \Gamma_w \}, \\ V_0 &= \{ \mathbf{u}_f \in [H^1(\Omega_f(t))]^3 : \mathbf{u}_f = 0 \text{ on } \Gamma_i \cup \Gamma_w \}, \\ P &= L^2(\Omega_f(t)). \end{aligned}$$

The weak form of the fluid problem reads: Find $\mathbf{u}_f \in V$ and $p_f \in P$ such that $\forall \phi_f \in V_0$ and $\forall \psi_f \in P$,

$$\begin{aligned} B_f(\{ \mathbf{u}_f, p_f \}, \{ \phi_f, \psi_f \}; \mathbf{x}_f) &= \rho_f \int_{\Omega_f(t)} \frac{\partial \mathbf{u}_f}{\partial t} \Big|_{\mathbf{Y}} \cdot \phi_f \, d\Omega - \int_{\Omega_f(t)} p_f (\nabla \cdot \phi_f) \, d\Omega \\ &+ \rho_f \int_{\Omega_f(t)} [(\mathbf{u}_f - \boldsymbol{\omega}_g) \cdot \nabla] \mathbf{u}_f \cdot \phi_f \, d\Omega + 2\mu_f \int_{\Omega_f(t)} \boldsymbol{\varepsilon}(\mathbf{u}_f) : \boldsymbol{\varepsilon}(\phi_f) \, d\Omega \\ &+ \int_{\Omega_f(t)} (\nabla \cdot \mathbf{u}_f) \psi_f \, d\Omega = 0, \end{aligned}$$

where $\varepsilon(\mathbf{u}_f) = (\nabla \mathbf{u}_f + \nabla \mathbf{u}_f^T)/2$.

The weak form of the domain movement problem reads: Find $\mathbf{x}_f \in Z$ such that $\forall \xi \in Z_0$,

$$B_m(\mathbf{x}_f, \xi) = \int_{\Omega_0} \nabla \xi : \nabla \mathbf{x}_f \, d\Omega = 0.$$

And the variational spaces are defined as

$$\begin{aligned} Z_0 &= \{\mathbf{x}_f \in [H^1(\Omega_0)]^3 : \mathbf{x}_f = 0 \text{ on } \Gamma_i \cup \Gamma_o \cup \Gamma_w\}, \\ Z &= \{\mathbf{x}_f \in [H^1(\Omega_0)]^3 : \mathbf{x}_f = \mathbf{x}_s \text{ on } \Gamma_w, \mathbf{x}_f = 0 \text{ on } \Gamma_i \cup \Gamma_o\}. \end{aligned}$$

We discretize the fully coupled problem in space with a finite element method, by using unstructured P1-P1 stabilized elements for the fluid, P1 elements for the structure and P1 elements for the fluid domain motion. We denote the finite element subspaces $X_h, V_h, V_{h,0}, P_h, Z_h, Z_{h,0}$ as the counterparts of their infinite dimensional subspaces. Because the fluid problem requires that the pair V_h and P_h satisfy the LBB inf-sup condition, additional SUPG stabilization terms are needed in the formulation with equal-order interpolation of the velocity and the pressure as described in [11, 12]. The semi-discrete stabilized finite element formulation for the fluid problem reads as follows: Find $\mathbf{u}_f \in V_h$ and $p_f \in P_h$, such that $\forall \phi_f \in V_{h,0}$ and $\forall \psi_f \in P_h$,

$$B(\{\mathbf{u}_f, p_f\}, \{\phi_f, \psi_f\}; \mathbf{x}_f) = 0,$$

with

$$\begin{aligned} &B(\{\mathbf{u}_f, p_f\}, \{\phi_f, \psi_f\}; \mathbf{x}_f) \\ &= B_f(\{\mathbf{u}_f, p_f\}, \{\phi_f, \psi_f\}; \mathbf{x}_f) + \sum_{K \in \mathcal{T}_f^h} (\nabla \cdot \mathbf{u}_f, \tau_c \nabla \cdot \phi_f)_K \\ &+ \sum_{K \in \mathcal{T}_f^h} \left(\frac{\partial \mathbf{u}_f}{\partial t} \Big|_{\mathbf{Y}} + (\mathbf{u}_f - \omega_g) \cdot \nabla \mathbf{u}_f + \nabla p_f, \tau_m ((\mathbf{u}_f - \omega_g) \cdot \nabla \phi_f + \nabla \psi_f) \right)_K, \end{aligned}$$

where $\mathcal{T}_f^h = \{K\}$ is the given unstructured tetrahedral fluid mesh, and τ_c and τ_m are stabilization parameters.

We form the finite dimensional fully coupled FSI problem as follows: Find $x_s \in X_h, \dot{x}_s \in X_h, u_f \in V_h, p_f \in P_h$ and $x_f \in Z_h$ such that $\forall \phi_s \in X_h, \forall \varphi_s \in X_h, \forall \phi_f \in V_{h,0}, \forall \psi_f \in P_h$, and $\forall \xi \in Z_{h,0}$,

$$B_s(\{x_s, \dot{x}_s\}, \{\phi_s, \varphi_s\}; \sigma_f) + B(\{u_f, p_f\}, \{\phi_f, \psi_f\}; x_f) + B_m(x_f, \xi) = 0. \quad (3)$$

The system (3) is further discretized in time with a second-order BDF2 scheme. Since the temporal discretization scheme is fully implicit, at each time step, we obtain the solution x^n at the n th time step from the previous two time steps by solving a sparse, nonlinear algebraic system

$$\mathcal{F}_n(x^n) = 0, \quad (4)$$

where x^n corresponds to the nodal values of the fluid velocity \mathbf{u}_f , the fluid pressure p_f , the fluid mesh displacement \mathbf{x}_f , the structure displacement \mathbf{x}_s and the structure velocity $\dot{\mathbf{x}}_s$ at the n th time step. For simplicity, we ignore the script n for the rest of the paper.

3 Newton-Krylov-Schwarz Method

In the Newton-Krylov-Schwarz approach, the nonlinear system (4) is solved via the inexact Newton method [8]. At each Newton step the new solution $x^{(k+1)}$ is obtained from the current solution $x^{(k)}$ by $x^{(k+1)} = x^{(k)} + \theta^{(k)}s^{(k)}$, where the step length $\theta^{(k)}$ is determined by a cubic line search technique. The Newton correction $s^{(k)}$ is approximated by solving a preconditioned Jacobian system $J_k M_k^{-1} M_k s^{(k)} = -\mathcal{F}(x^{(k)})$ with GMRES, where M_k^{-1} is a one-level restricted additive Schwarz preconditioner [5].

To define the domain decomposition preconditioner, we first partition the finite element mesh (which consists of the meshes for all components of the coupled system) into non-overlapping subdomains Ω_ℓ^h , $\ell = 1, \dots, N$, where the number of subdomain N is always the same as the number of processors np . Then, each subdomain Ω_ℓ^h is extended to an overlapping subdomain $\Omega_\ell^{h,\delta}$. Note that the decomposition of the mesh is completely independent of which physical variables are defined on a given mesh point. The number of variables at a given mesh point is considered for the purpose of load balancing. The so-called one-level restricted additive Schwarz preconditioner is defined by

$$M_k^{-1} = \sum_{\ell=1}^N (R_\ell^0)^T J_\ell^{-1} R_\ell,$$

where R_ℓ^0 and R_ℓ are restrictions to the degrees of freedom in the non-overlapping subdomain Ω_ℓ^h and the overlapping subdomain $\Omega_\ell^{h,\delta}$, respectively. J_ℓ is a restriction of the Jacobian matrix defined by $J_\ell = R_\ell J_k R_\ell^T$.

4 Numerical Results

Our algorithm is implemented using PETSc [1]. All computations are performed on an IBM BlueGene/L supercomputer.

A benchmark 3D FSI problem is used to study the efficiency and performance of our fully-coupled algorithm and software. The geometry consists of a straight cylinder representing the fluid domain with length 5 cm and radius 0.5 cm, and the surrounding structure with thickness 0.1 cm. A constant traction $\sigma_f \cdot \mathbf{n} = 1.33 \cdot 10^4$ dynes/cm² is imposed on the inlet boundary for 3 ms. A zero traction condition is applied to the fluid at the outlet boundary. The fluid is characterized with viscosity $\mu_f = 0.03$ poise, and density $\rho_f = 1.0$ g/cm³. The Young's modulus $E = 3 \cdot 10^6$ g/(cm s²), the Poisson ratio $\nu_s = 0.3$, and the structure density $\rho_s = 1.2$ g/cm³ are the parameters of the structure model.

The fluid and the structure are initially at rest and the simulation is run on a mesh with $2.41 \cdot 10^6$ elements and $3.08 \cdot 10^6$ degrees of freedom, for a total time of 10 ms with a time step size $\Delta t = 0.1$ ms. The simulation proceeds to the next time step when the residual of the nonlinear system is less than 10^{-6} . In Fig. 1, we show the computed fluid pressure and the structure deformation at $t = 2.5, 5.0, 10.0$ ms. Our results are similar to the published results in [7, 9]. We observe that the pressure wave propagates along the cylinder and reaches the end of the cylinder at $t = 10.0$ ms. The wall structure deforms in response to the propagation of the wall pressure, which is a key feature of the fluid-structure interaction.

The strong scalability of the algorithm is presented in Table 1. The results show superlinear scalability for a range of problem sizes and with up to 2,048 processors. It is worth noting that the growth in GMRES iterations for large processor counts may be a problem if we consider to solve the problem on a much larger mesh and with a larger number of processors. In those situations, one possible solution to improve the scalability is the use of a multilevel preconditioner.

Our algorithm is quite robust with respect to physical parameters. In some FSI methods, the convergence becomes difficult to achieve if the density of the fluid and the structure are close to each other. According to Table 2, our solver performs quite well for a wide range of fluid density and structure density.

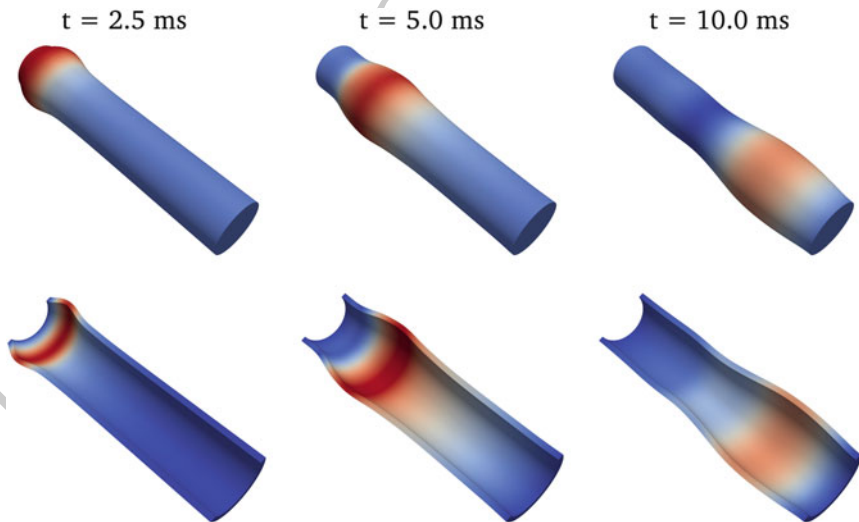


Fig. 1. Pressure wave propagation and structure deformation. The deformation is amplified by a factor of 12 for visualization purpose only

DOF	np	Newton GMRES time (s)		
$1.24 \cdot 10^6$	256	2.0	41.60	218.03
	512	2.0	49.85	87.53
	1024	2.0	55.65	37.88
$3.07 \cdot 10^6$	512	2.0	57.60	442.44
	1024	2.0	67.15	152.16
	2048	2.0	77.55	65.64

Table 1. Performance with respect to the number of processors for two different mesh sizes. “ np ” denotes the number of processors. “Newton” denotes the average Newton iteration per time step. “GMRES” denotes the average GMRES iterations per Newton step. “time” refers to the average compute time, in seconds, per time step.

ρ_f	ρ_s	Newton GMRES time (s)		
1.0	0.1	2.0	71.65	89.94
1.0	1.0	2.0	49.85	87.53
1.0	10.0	2.0	53.90	88.07
1.0	100.0	2.0	61.75	88.84
0.01	1.0	2.0	124.60	96.75
0.1	1.0	2.0	60.90	88.77
10.0	1.0	2.0	60.85	88.79

Table 2. Different combinations of fluid density ρ_f and structure density ρ_s . μ_f is kept at 0.03 poise. The tests are run for a problem with $1.25 \cdot 10^6$ unknowns and 512 processors.

5 Conclusion

164

In this paper, we developed and studied a parallel scalable overlapping Schwarz domain decomposition method for solving the fully coupled fluid-structure interaction system in 3D. Our algorithm is shown to be scalable on a large scale supercomputer and robust with respect to several important physical parameters.

165

166

167

168

Bibliography

169

- [1] S. Balay, K. Buschelman, V. Eijkhout, W. Gropp, D. Kaushik, M. Knepley, L. Curfman McInnes, B. Smith, and H. Zhang. PETSc User Manual. Technical report, Argonne National Laboratory, 2010. 170
171
172
- [2] A. T. Barker and X.-C. Cai. Scalable parallel methods for monolithic coupling in fluid-structure interaction with application to blood flow modeling. *J. Comput. Phys.*, 229:642–659, 2010. 173
174
175
- [3] A. T. Barker and X.-C. Cai. Two-level Newton and hybrid Schwarz preconditioners for fluid-structure interaction. *SIAM J. Sci. Comput.*, 32:2395–2417, 2010. 176
177
178

- [4] Y. Bazilevs, V. M. Calo, T. J. R. Hughes, and Y. Zhang. Isogeometric fluid-structure interaction: Theory, algorithms and computations. *Comput. Mech.*, 43:3–37, 2008. 179–181
- [5] X.-C. Cai and M. Sarkis. A restricted additive Schwarz preconditioner for general sparse linear systems. *SIAM J. Sci. Comput.*, 21:792–797, 1999. 182–183
- [6] P. Causin, J. F. Gerbeau, and F. Nobile. Added-mass effect in the design of partitioned algorithms for fluid-structure problems. *Comput. Methods Appl. Mech. Engrg.*, 194:4506–4627, 2005. 184–186
- [7] S. Deparis, M. Discacciati, G. Fourestey, and A. Quarteroni. Fluid-structure algorithms based on Steklov-Poincaré operators. *Comput. Methods Appl. Mech. Engrg.*, 195:5797–5812, 2006. 187–189
- [8] S. C. Eisenstat and H. F. Walker. Choosing the forcing terms in an inexact Newton method. *SIAM J. Sci. Comput.*, 17:16–32, 1996. 190–191
- [9] M. A. Fernandez and M. Moubachir. A Newton method using exact Jacobians for solving fluid-structure coupling. *Comput. Struct.*, 83:127–142, 2005. 192–193
- [10] L. Formaggia, J. F. Gerbeau, F. Nobile, and A. Quarteroni. On the coupling of 3D and 1D Navier-Stokes equations for flow problems in compliant vessels. *Comput. Methods Appl. Mech. Engrg.*, 191:561–582, 2001. 194–196
- [11] L. P. Franca and S. L. Frey. Stabilized finite element methods. II. The incompressible Navier-Stokes equations. *Comput. Methods Appl. Mech. Engrg.*, 99:209–232, 1992. 197–199
- [12] T. Tezduyar and S. Sathe. Stabilization parameters in SUPG and PSPG formulations. *J. Comput. Appl. Mech.*, 4:71–88, 2003. 200–201